*Desalination and Water Treatment*
www.deswater.com
doi: 10.5004/dwt.2020.24714

173 (2020) 49–56
January

# Removal of graphene oxide from water and wastewater using coagulation–flocculation

Natália R. Guimarães[a,*], Hang N. Nguyen[b], Sidney S. Ferreira Filho[a], Debora F. Rodrigues[b]

[a]*Department of Hydraulic and Environmental Engineering, University of Sao Paulo, São Paulo, Brazil, Tel. +55 (11) 3091 5444; email: nati_guimaraes@yahoo.com.br (N.R. Guimarães), Tel. +55 (11) 3091 5222; email: ssffilho@usp.br (S.S.F. Filho)*
[b]*Department of Civil and Environmental Engineering, University of Houston, Houston, Texas, USA, Tel. +1 (713) 743-1495; emails: dfrigirodrigues@uh.edu (D.F. Rodrigues), huongem@hotmail.com (H.N. Nguyen)*

Received 21 May 2018; Accepted 24 July 2019

**ABSTRACT**

The present study evaluated the removal of graphene oxide (GO) concentrations of 1, 5 and 10 mg $L^{-1}$ on water and wastewater secondary effluent from conventional activated sludge via coagulation–flocculation with different concentrations of iron chloride and polyaluminum chloride (PAC) as coagulants. UV–Vis spectroscopy was used to measure GO concentrations in the water and secondary effluent solutions before and after the coagulation–flocculation treatment. Fourier transform infrared (FTIR) analyses were used to evaluate the presence of GO in the residual sludge. The results showed that the coagulation–flocculation process was effective in removing GO from both water and wastewater secondary effluents. In DI water solution, iron chloride showed a higher removal, but with high standard deviation values, meaning an instability of results. PAC results were more stable. For the wastewater GO solution, PAC showed better results on all GO concentrations and coagulant concentrations. FTIR results showed the presence of GO in the settled sludge from both water and wastewater solutions; zeta potential analyses showed that metal coagulants ferric chloride and PAC have an impact on zeta potential of GO particles in DI water solution elucidating that the main mechanism for GO removal was sweep flocculation.

*Keywords:* Graphene oxide; Wastewater treatment; Coagulation–flocculation process; PAC; Iron chloride; UV–Vis

## 1. Introduction

In several countries, the reuse of secondary effluents from wastewater treatment plants (WWTP) is a common strategy to minimize the consumption of drinking water for purposes such as public road washes and industrial use. Typically, after the wastewater secondary treatment, some WWTPs have introduced additional treatment techniques, such as chemical coagulation followed by flocculation, filtration and chemical oxidation to further clean the effluent for reuse. Studies have demonstrated that the use of coagulation, flocculation and sedimentation led to the effective removal of suspended solids and natural organic and inorganic matter during traditional water and wastewater treatment processes [1–5].

Manufactured nanomaterials (NM) have been an object of research since fullerene, the first manufactured NM was produced, in 1985. Carbon nanotubes, derivative from fullerene, were the next [6]. Nanoparticles (NP) of graphene oxide (GO) originated from graphite oxide and are promising NP, with different applications [7]. Because of the unique mechanical, electrical, catalytic and optical properties [8] of graphene-based materials, a global market growth of $675 million is expected by 2020 [9–11].

The wide use of manufactured NM and NP brings to attention the fact that they may eventually damage the environment [12]. Given the increasing production of graphene-based NMs and their incorporation in consumer products,

* Corresponding author.

there is a high probability that they will be released into WWTPs [11,13] and further into the environment. There are no records of the exact concentration of GO expected in WWTPs, but some authors have been working with modeling [12] and testing [13] to find probable concentrations.

As previously mentioned, studies have evaluated the impact of NMs on the environment [6,14,15] and on WWTPs [16–24].

In the case of nanomaterials (NMs) released from consumer products, there is still the need to evaluate how NM can be removed to control environmental and health risks associated with its exposure [25]. Studies have addressed the removal of NM from water and wastewater using filtration [26] and coagulation–flocculation processes [27–32].

Considering that coagulation combined with flocculation is the most widely used method to treat final WWTP effluents for reuse, it is important to understand how this process interacts with NM. Coagulation–flocculation is a common process used to remove colloidal particles. The concept of colloidal particles can include NP and, consequently, the coagulation–flocculation process is able to remove NP by the same mechanisms that affect colloidal particles [29].

Still, dissolved organic matter can adsorb on the surface of NMs, such as carbon-based NMs, thereby changing their surface physical–chemical properties [33–35].

Thus, it is vital to perform systematic investigations on how conventional water treatment technologies remove particles from complex water matrices (i.e., wastewater), specially targeting the evaluation of nanoparticles removal [11,19,25,27].

Honda et al. [27] considered coagulation and flocculation a good mechanism to remove $TiO_2$ particles from both surface and groundwater. In their study on the removal of CNT (carbon nanotubes) and $TiO_2$ NP dispersed in humic acid with aluminum coagulant, Zhang et al. [36] verified that particle size influences the coagulant concentration and NP removal and that the coagulation process conditions, such as pH and ionic strength are important to obtain better removal results. Recently, Popowich et al. [29] reviewed the results of studies applying coagulation to remove NP from water matrices, pointing out difficulties and suggesting focus on the concentration range and types of toxic NM.

Only few studies found in the literature address GO as a pollutant and evaluate its consequences for microorganisms, such as the ones in WWTP [37], and how it behaves under coagulation–flocculation, in the case of water treatment or wastewater reuse. Thus, giving the lack of information on GO behavior and interaction with coagulants, this study investigated the removal of graphene oxide (GO) with a chemical coagulation–flocculation process in clean water and wastewater secondary effluent, evaluating the concentration of GO using UV–Vis.

## 2. Experimental protocols

### 2.1. Water samples GO and chemicals solutions

The study was conducted using distilled water and secondary effluent as a solution for GO removal. Characteristics for secondary effluent are provided in Supporting Information.

Graphene oxide was synthesized from graphite (<20 μm, Sigma-Aldrich, USA). Methods for the synthesis and characterization are provided in the Supporting Information.

The stock solution containing 1,000 mg $L^{-1}$ GO used in this study was prepared according to a modified methodology previously described [38]. GO concentrations of 1, 5 and 10 mg $L^{-1}$ were used for the experiments. More information about GO UV–Vis detection and calibration curve is supplied in Supporting Information.

For the coagulation–flocculation assay, two coagulants were used: polyaluminum chloride (PAC) (Kemira Chemicals PAX-XL8, 70% basicity) and ferric chloride hexahydrate (Sigma-Aldrich), at three different concentrations: 1.87, 3.74 and 5.61 mg Al $L^{-1}$ and 2.07, 4.14 and 6.21 mg Fe $L^{-1}$. Details of the coagulant solutions and chemistry are provided in Supporting Information.

### 2.2. Coagulation–flocculation assays

The coagulation–flocculation assays were conducted at room temperature using the jar test procedure. The jar test procedure was performed with a laboratory stirrer (Jar Tester, Phipps and Bird, Inc., Richmond, VA) composed of six flat paddles attached to a rotation system with a jar with a 2 L volume capacity. For the experiments, only one jar was used at a time. Experiments were made in triplicates to guarantee a good observation of removal and results.

The test consists of three parts: (1) fast mixing, inducing coagulation; (2) slow mixing, inducing flocculation and (3) settling, allowing particles to settle at the bottom of the jar, separating from the treated liquid phase. The fast mixing was performed to ensure a velocity gradient equal to or greater than 1,000 $s^{-1}$ [39]. For that purpose, the jar test rotation was kept constant at 100 rpm for 60 s. After the fast mixing step, the rotation was reduced to 20 rpm for 15 min to guarantee a speed gradient of around 30 $s^{-1}$. The flocculation velocity gradient was based on typical reactor designs used in water treatment plants [40]. After 15 min of flocculation, the equipment was turned off and a 5-min sedimentation step was conducted. After sedimentation, a 500-mL sample from the supernatant was collected to measure the GO concentration with the UV–Vis spectrophotometer.

The procedure was repeated in triplicates for both coagulants (ferric chloride and PAC) in each proposed dosage (2.07, 4.14 and 6.21 mg Fe $L^{-1}$ and 1.87, 3.74 and 5.61 mg Al $L^{-1}$) for each concentration of GO (1, 5 and 10 mg $L^{-1}$ GO) present in DI water or secondary effluent. A control without any coagulant (0 mg $L^{-1}$) was used as well. To ensure that the jar tests were conducted within a neutral pH range (6.0 to 7.5), a pH meter was inserted in the jar and the pH was controlled by adding NaOH 0.1 M or HCl 0.1 M during the experiment. The pH range was chosen based on literature about coagulation process using metal salts coagulants

In addition to determining the best coagulant and the effect of the coagulant concentration, we also examined the interactions of GO with the coagulants through zeta potential (ZP) analysis. The ZP measurement was conducted with GO suspended in DI water solution using the jar test procedure method as described above. The ZP of the GO solution with every concentration proposed (1, 5 and 10 mg $L^{-1}$ GO) was measured before the jar test procedure started using a 10 mL

sample of the solution and inserting it in the ZP equipment (zeta potential/particle sizer, NICOMP 380ZLS, California, USA). After 30 s from addition of coagulant, at the jar test fast mixing step, a 10-mL sample was taken from the solution and its ZP was analysed.

### 2.3. Estimation of GO removal by coagulation–flocculation

In order to determine the removal of GO from the coagulation–flocculation solutions, the quantification of the residual GO in the post-treated water was determined using UV–Vis based on the calibration curve. The following equation was obtained to determine the GO concentration: GO (mg $L^{-1}$) = 0.0361$x$ + 0.0057, where $x$ = absorbance result; $R^2$ = 0.9976. Background subtraction, using DI water, prior to the addition of GO to the samples was necessary in order not to underestimate or overestimate the GO in the final effluent.

The removal of GO from the wastewater was further confirmed by Fourier transform infrared (FTIR) analyses of the residual sludge produced in the jar test. Protocol followed was according to Bykkam et al. [41]. The residual sludge sample from each jar test with the best GO removals had their sludge collected from the bottom of the jar with a micro pipette and filtered through a glass fiber filter (0.45 microns). The filters containing the sludge were subjected to FTIR analyses to determine the presence of GO by identifying the characteristic GO functional groups. For this and to exclude any interference of any other substances with the water or with the coagulants, five controls were used. The controls were: the bare filter used for filtrating the sludge; pure GO deposited on the filters; ferric chloride coagulant deposited on the filter; PAC coagulant deposited on the filter; and the retentate of the secondary effluent used in this study.

## 3. Results and discussion

### 3.1. Graphene oxide removal from DI water

Initial experiments to understand the interactions of GO with ferric chloride and PAC coagulants were performed with DI water (simple matrix). Fig. 1 shows the mean values of removal percentage for each GO concentration with coagulation with different coagulant concentration. Ferric chloride, for 10 ppm GO, removed from 55% to 60% with 2.07 mg Fe $L^{-1}$; 33% to 92% with 4.14 mg Fe $L^{-1}$; and 70% to 82% with 6.21 mg Fe $L^{-1}$ (Fig. 1a). For 5 ppm GO, ferric chloride coagulant removed from 22% to 52% with 2.07 mg Fe $L^{-1}$; 3% to 57% with 4.14 mg Fe $L^{-1}$; and 0%–48% with 6.21 mg Fe $L^{-1}$ (Fig. 1a).

PAC coagulant, for 10 ppm GO, removed 55%–78% with 1.87 mg Al $L^{-1}$; 75%–92% with 3.74 mg Al $L^{-1}$; and 47%–76% with 5.61 mg Al $L^{-1}$ (Fig. 1b). For 5 ppm GO, PAC coagulant removed from 74% to 93% with 1.87 mg L Al $L^{-1}$; 87% with 3.74 mg Al $L^{-1}$; and with 5.61 mg Al $L^{-1}$, there was no removal (Fig. 1b).

High standard deviations were observed in the removal of GO from DI water solution. This shows that the composition of water solution may influence the GO removal using coagulants [42]. One hypothesis may be that GO forms suspensions in water with different sizes of NP agglomerates; being the only particle in solution contact with the coagulant is less stable.

The higher percentage removal of GO using PAC and not needing to adjust the coagulant concentration makes PAC a more attractive coagulant for GO removal from water. The results showed that solutions of 1 mg $L^{-1}$ GO in DI water were not removed by any of the PAC concentrations investigated (data not shown). This can be explained by the fact that, at lower concentrations, suspended particles destabilization requires charge neutralization [40], and the ideal coagulant dosage for charge neutralization at lower particle concentrations is hard to be achieved. Typically, lower particle concentrations require lower coagulant concentrations, which prevent the formation of metal hydroxide precipitates and particle removal by sweep flocculation. Therefore, the removal of suspended GO in lower concentrations can be challenging, especially if GO is the only suspended particle in the solution.

### 3.2. Zeta potential measurements

In the present study, we evaluated the changes in the ZP of GO in DI water solutions before and after the application of coagulants (Fig. 2).

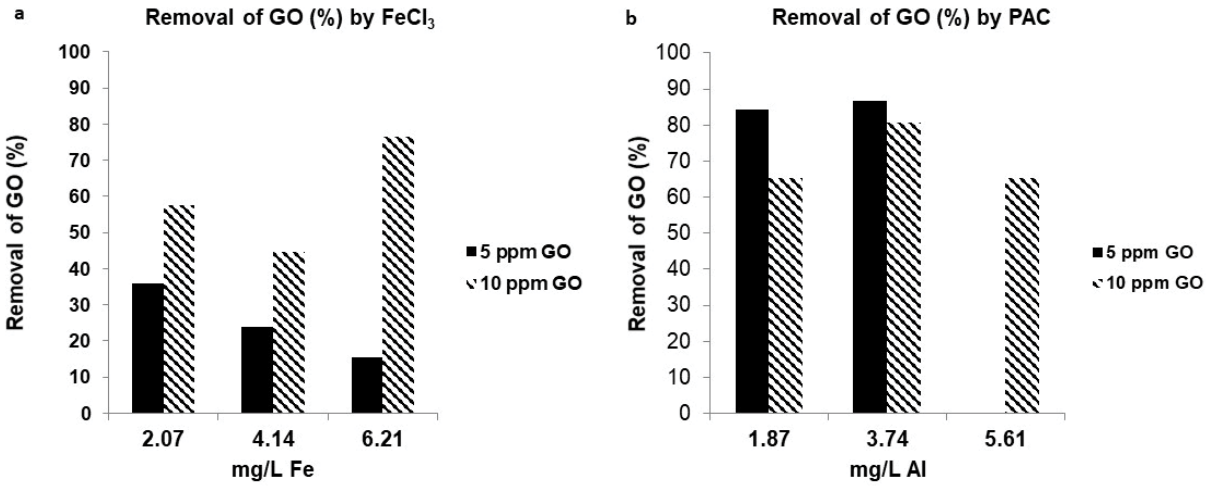


Fig. 1. Percentage removal of GO in DI water by (a) iron chloride coagulant and (b) PAC coagulant.

The GO solution without coagulant presented a negative ZP (around –20 mV) at neutral pH. This is observed because of the deprotonation of the GO functional groups at this pH [43]. When the ZP was negative, the particles were chemically stable and remained in suspension. In the coagulation step, the aggregation of the particles is necessary for particle removal. Therefore, in this study, in most measurements, the increasing concentration of coagulant reduced the negative charges of GO allowing the particles to aggregate and settle. In some cases, the coagulant led to particle charge change from negative to positive (Fig. 3) still allowing particles to aggregate and to remove GO. This phenomenon was observed in the samples containing 5 mg $L^{-1}$ GO treated with 20 mg $L^{-1}$ of $FeCl_3$ and in samples of 10 mg $L^{-1}$ GO treated with 10 and 30 mg $L^{-1}$ of $FeCl_3$ (Fig. 2a). This behavior can also be observed with colloidal particles present in natural waters [40].

In the case of PAC, the charge inversion of the ZP was observed in the samples containing 5 mg $L^{-1}$ GO treated with 10 and 20 mg $L^{-1}$ of PAC and 10 mg $L^{-1}$ GO treated with 20 and 30 mg $L^{-1}$ of PAC (Fig. 2b). In this case, the dominant removal mechanism was probably sweep flocculation, since charge neutralization was not achieved in most samples [40]. The only sample that showed charge neutralization (ZP ≈ zero) was 5 mg $L^{-1}$ GO treated with 10 mg $L^{-1}$ of $FeCl_3$ (ZP = –0.3 mV), which resulted in a GO removal of 36%.

As the coagulants, GO also has surface charge; hence, surface potential plays an essential role in the interactions of nanoparticles with each other and other chemicals/molecules. The nanoparticle aggregates observed herein presented similar behavior to that of colloids; however, the extent to which GO-coagulant aggregates behave from these previously studied colloids is still unknown. It is possible that the interaction energies are very different and more complex than the ones currently observed in the colloid literature [44].

### 3.3. Graphene oxide removal in secondary effluent

The same coagulants investigated with DI water were also used to compare the removal of GO in a wastewater secondary effluent. The results for GO removal by ferric chloride and PAC are presented in Fig. 3.

Ferric chloride, for 10 ppm GO, removed from 65% to 70% with 2.07 mg Fe $L^{-1}$; 60% to 65% with 4.14 mg Fe $L^{-1}$; and 53% to 55% with 6.21 mg Fe $L^{-1}$ (Fig. 3a). For 5 ppm GO, ferric chloride coagulant removed from 8% to 11% with 2.07 mg Fe $L^{-1}$; 37% to 40% with 4.14 mg Fe $L^{-1}$; and 17% with 6.21 mg Fe $L^{-1}$ (Fig. 3a).

PAC coagulant, for 10 ppm GO, removed from 82% to 86% with 1.87 mg L Al $L^{-1}$; 89% to 93% with 3.74 mg Al $L^{-1}$; and 98% with 5.61 mg Al $L^{-1}$ (Fig. 3b). For 5 ppm GO, PAC coagulant removed from 72% to 77% with 1.87 mg L Al $L^{-1}$; 89% to 100% with 3.74 mg Al $L^{-1}$; and 97% to 100% with 5.61 mg Al $L^{-1}$(Fig. 3b). For 1 ppm GO, PAC coagulant removed from 94% to 96% with 1.87 mg L Al $L^{-1}$; 96% to 98% with 3.74 mg Al $L^{-1}$; and 97% to 100% with 5.61 mg Al $L^{-1}$ (Fig. 3b).

The standard deviation of GO removal from wastewater solution was very low.

As in the DI water, the PAC results seem to make it a more attractive coagulant for GO removal from WWTPs due to a higher percentage removal. PAC was developed to increase the concentration of the most efficient species, $Al_{13}$ (simplified form of $AlO_4Al_{12}(OH)_{24}$), because of its high stability and positive electric charge [45]. This coagulant is known for its stability after dilution, low turbidity production and stability over a wider pH range [46].

In complex matrices, such as secondary effluents, GO is known to interact with other colloidal particles, which would change the surface chemistry of GO [11]. That would in return affect the interactions of the nanomaterials with the coagulants. The details of how the interaction of GO with the coagulants takes place are yet not completely understood; however, previous studies with other nanomaterials have shed some light on the potential mechanisms of interactions.

Observations made about physical–chemical properties and concentrations of colloids and organic matter in the water [14,47,48] can be taken into consideration in the results of the present study. We observed that the floc formation

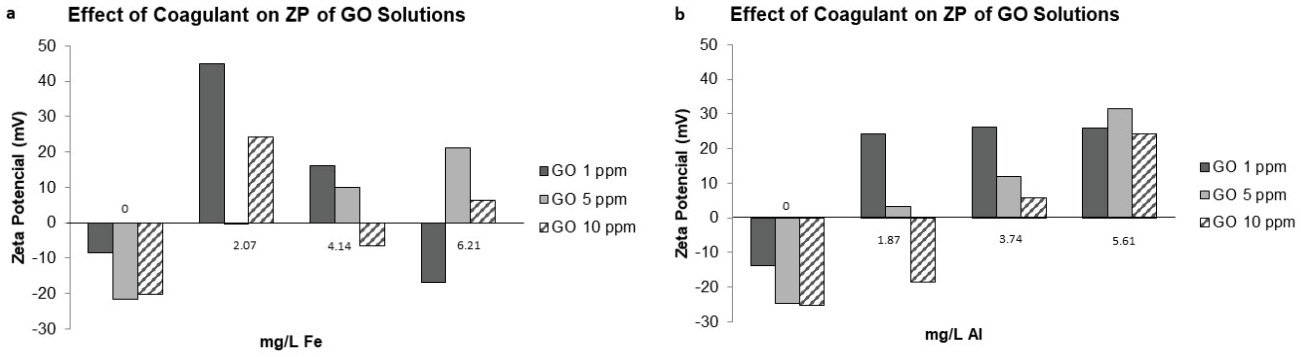


Fig. 2. Zeta potential analyses for GO solution in DI water in the presence of different concentrations of coagulants (a) iron chloride coagulant and (b) PAC coagulant. In the graph, "0" (zero) concentration of coagulants correspond the ZP measurement of GO before the addition of the coagulants. Different patterns on columns indicate GO concentration (ppm) according to subtitle box, axis "X" indicates coagulant concentration in mg $L^{-1}$.

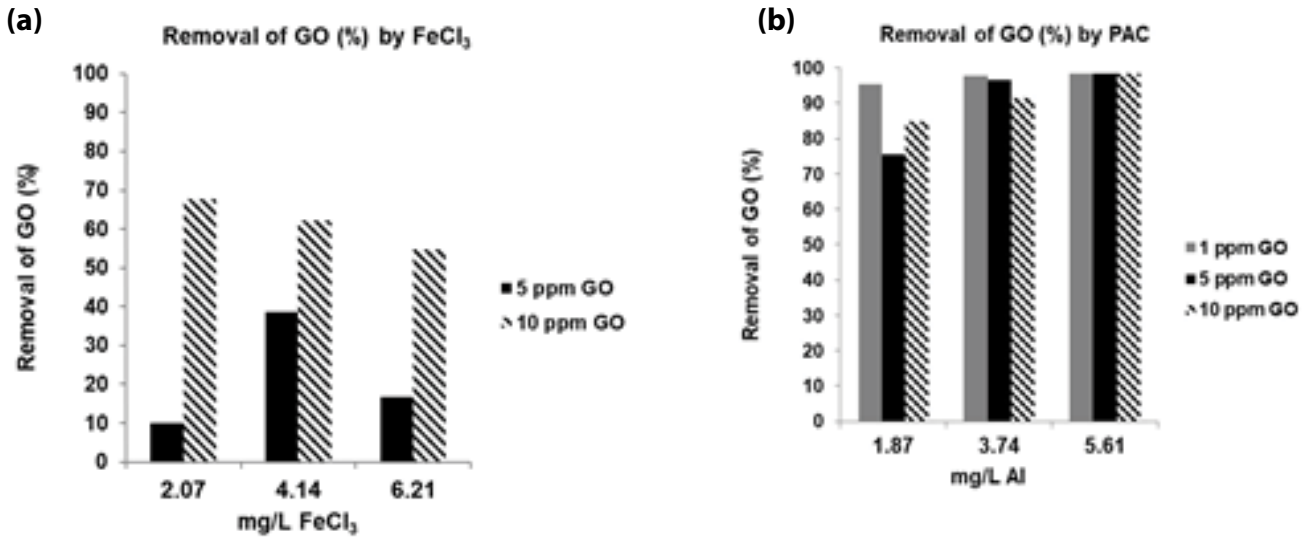


Fig. 3. Percentage removal of GO in secondary effluent by different coagulants at different concentrations: (a) iron chloride and (b) PAC.

appeared to be stabler in the presence of particles in the secondary effluent GO solution. Furthermore, the flocs presented more nucleation capacity due to the presence of other colloidal particles in the secondary effluent, besides GO. In the secondary effluent, it is also likely that some organic molecules adsorbed to the GO surface changing its surface chemistry since the experiments were conducted at neutral pH (6.5 < pH > 7.5), which could have also explained the higher removal of GO in secondary effluent than in the DI water. Additionally, in agreement with the studies cited above [10,14,46], the secondary effluent solution typically possesses high ionic strength, which makes GO more likely to flocculate by heteroaggregation with other organic suspended particles. According to Honda et al. [27], GO adsorption capacities in the presence of dissolved monovalent (NaCl) and divalent ($CaCl_2$) salts decrease. This reduction of adsorbed protein in the presence of ions was also observed in other studies as the result of double layer interactions with both particles [49]. The positive cations balance the negative charges on GO, reducing the interaction strength between GO and the material tested.

The literature about coagulation–flocculation mechanisms points out that the condition necessary to obtain charge neutralization is using, at neutral pH, very low metal coagulants concentration (micromoles $L^{-1}$) so that the hydrated metal and its various hydrolyzed species, that is, metal coagulants soluble species, are present. Usually, in water treatment facilities, the coagulant dosage is higher than that cited to obtain charge neutralization, and still particle removal is very efficient. The explanation can be found in the sweep coagulation mechanism, whereby particles present in the water solution are incorporated in hydroxides precipitates and removed from suspension (sweeping) [50]. Based on the information above, it can be concluded that the dominant GO removal mechanism observed was sweep coagulation. This conclusion agrees with the findings by Honda et al. [27] for $TiO_2$ NPs.

It is important to emphasize that the ideal choice of coagulant and parameters for NP removal are dependent on the type of NP and on the physical–chemical characteristics of the liquid phase.

### 3.4. Presence of GO on the sludge after flocculation

FTIR spectroscopy (Nicolet iS10, Thermo Scientific, USA) was used for analyzing the settled sludge obtained after the interaction of secondary effluent GO solution with coagulants during the jar test procedure.

Figs. 4 and 5 show the results from FTIR analyses for 5 and 10 mg $L^{-1}$ GO in secondary effluent solution, respectively. Both the figures also show the results from control analyses.

In Fig. 4, distinctive peak "C=O" at GO control sample is seen at 1,728 $cm^{-1}$. This peak appeared in the settled sludge as a very small shoulder in samples with PAC 30 mg $L^{-1}$, $FeCl_3$ 10 and 20 mg $L^{-1}$. These samples presented 98.3% (±1.1), 67.7% (±2.0), 62% (±2.3), respectively. The small peak size in sludge samples from the jar test is due to the low concentration of GO in the samples. The second peak observed in the GO control were "C=C"; this peak was slightly shifted from 1,628 to 1,641 $cm^{-1}$ in the wastewater GO solutions and increased due to the interaction of GO with other chemical constituents present in the secondary effluent. This shift was observed previously in the presence of organic matter [10].

The small peak "C–H" (1,370–1,350 $cm^{-1}$), which appeared in both GO and secondary effluent control samples were present in all settled sludge samples after the jar test.

The observations made for 5 mg $L^{-1}$ of GO wastewater solution apply to 10 mg $L^{-1}$ GO wastewater solution. The low concentration of GO and the interaction with organic matter also caused the small shoulder at the "C=O" peak and the shifting at the "C=C" peak. Yet peaks were slightly narrower in 10 mg $L^{-1}$ of GO wastewater solution.

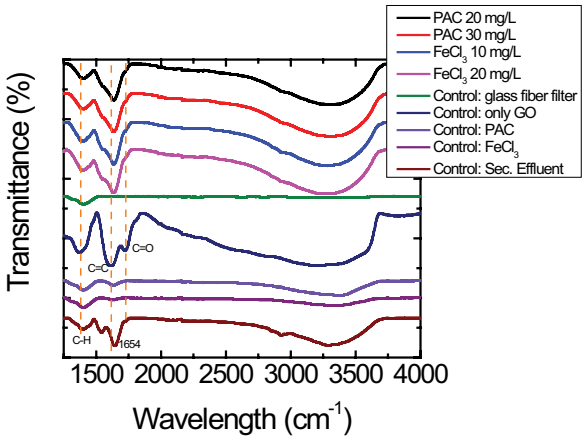


Fig. 4. FTIR of the sludge after coagulation of the secondary effluent samples with GO at 5 mg $L^{-1}$ and controls.

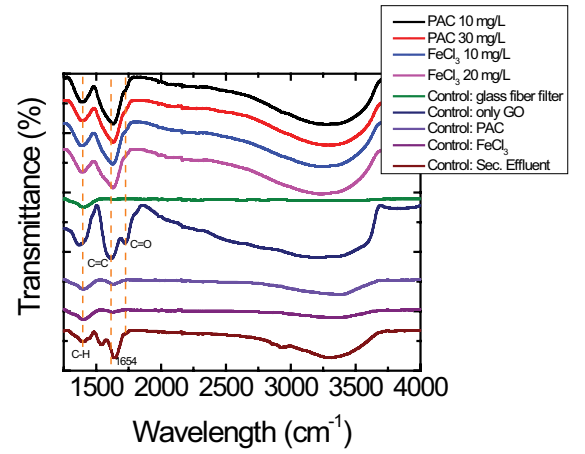


Fig. 5. FTIR of the sludge after coagulation of the secondary effluent samples with GO at 10 mg $L^{-1}$ and controls.

The presence of characteristic GO peaks in the settled sludge samples collected after the jar test procedure corroborate the UV–Vis results showing the removal of GO from the wastewater solution.

FTIR is a qualitative analysis, and from the results of this study, it is capable of detecting GO in wastewater solution. Still, a more accurate protocol can be developed to fully identify the peaks of GO in its interaction with organic matter.

## 4. Conclusions

The present study evaluated the removal of graphene oxide in different concentrations from water and conventional activated sludge's secondary effluent via coagulation–flocculation with different concentrations of coagulants. To evaluate de GO removal, UV–Vis spectroscopy was used to measure GO concentrations before and after the coagulation–flocculation treatment. FTIR analyses were used to evaluate the presence of GO in the residual sludge and zeta potential analyses were used to elucidate coagulation mechanisms on GO removal.

Based on the findings of the present study, it can be concluded that GO particles can be removed from water and wastewater by coagulation–flocculation process.

Based on the results, PAC presented better results in GO removal from both water and wastewater solutions and, in general, it can be said that metal coagulants, such as ferric chloride and PAC, have an impact on ZP of GO particles in DI water solution elucidating the main mechanism for GO removal, sweep flocculation. FTIR analyses showed GO in settled sludge, but at very small peaks, still showing the GO coagulation with metal salts.

Authors find that there is the need for a more accurate study on GO interaction with organic matter in order to better evaluate its removal from complex solutions such as wastewater. Still, authors suggest that not only GO but also the NP should be investigated in order to better understand the impact of water and wastewater treatment of its behavior.

## Acknowledgments

This project was partially supported by the NSF Career Award Nanohealth #104093. Natália R. Guimarães would like to acknowledge CNPq for the sandwich scholarship to do this work at the University of Houston (nº: 249076/2013-6).

## References

[1] J.R. Domínguez, J.B. de Heredia, T. González, F. Sanchez-Lavado, Evaluation of ferric chloride as a coagulant for cork processing wastewaters. Influence of the operating conditions on the removal of organic matter and settleability parameters, Ind. Eng. Chem. Res., 44 (2005) 6539–6548.

[2] J. Beltrán-Heredia, J. Sánchez-Martín, C. Solera-Hernández, Anionic surfactants removal by natural coagulant/flocculant products, Ind. Eng. Chem. Res.. 48 (2009) 5085–5092.

[3] H. Zhao, H. Liu, C. Hu, J. Qu, Effect of aluminum speciation and structure characterization on preferential removal of disinfection byproduct precursors by aluminum hydroxide coagulation, Environ. Sci. Technol., 43 (2009) 5067–5072.

[4] J. Duan, S. Shao, Ya-Li, L. Wang, P. Jiang, B. Liu, Polylactide/graphite nanosheets/MWCNTs nanocomposites with enhanced mechanical, thermal and electrical properties, Iran. Polym. J., 21 (2012) 109–120.

[5] E.-S. Kim, Y. Liu, M. Gamal El-Din, Evaluation of membrane fouling for in-line filtration of oil sands process-affected water: the effects of pretreatment conditions, Environ. Sci. Technol., 46 (2012) 2877–2884.

[6] S.J. Klaine, P.J.J. Alvarez, G.E. Batley, T.F. Fernandes, R.D. Handy, D.Y. Lyon, S. Mahendra, M.J. McLaughlin, J.R. Lead, Nanomaterials in the environment: behavior, fate, bioavailability and effects, Environ. Toxicol. Chem., 27 (2008) 1825.

[7] D.R. Dreyer, S. Park, C.W. Bielawski, R.S. Ruoff, The chemistry of graphene oxide, Chem. Soc. Rev., 39 (2010) 228–240.

[8] X. Huang, Z. Yin, S. Wu, X. Qi, Q. He, Q. Zhang, Q. Yan, F. Boey, H. Zhang, Graphene-based materials: synthesis, characterization, properties, and applications, Small, 7 (2011) 1876–1902.

[9] S. Clark, G.G. Mallick, Global Graphene Market (Product Type, Application, Geography) - Size, Share, Global Trends, Company Profiles, Demand, Insights, Analysis, Research, Report, Opportunities, Segmentation and Forecast, 2013 - 2020, Allied Market Research, 2014. Available at: https://www.google.com.br/search?hl=pt-BR&q=S.+Clark,+G.G.+Mallick,+Global+Graphene+Market+(Product+Type,+Application,+Geography)+-+Size,+S

hare,+Global+Trends,+Company+Profiles,+Demand,+Insights,+Analysis,+Research,+Report,+Opportunities,+Segmentation+and (Accessed January 18, 2018).
[10] S.C. Smith, D.F. Rodrigues, Carbon-based nanomaterials for removal of chemical and biological contaminants from water: a review of mechanisms and applications, Carbon N. Y., 91 (2015) 122–143.
[11] F. Ahmed, D.F. Rodrigues, Investigation of acute effects of graphene oxide on wastewater microbial community: a case study, J. Hazard. Mater., 256–257 (2013) 33–39.
[12] F. Gottschalk, T. Sun, B. Nowack, Environmental concentrations of engineered nanomaterials: review of modeling and analytical studies, Environ. Pollut., 181 (2013) 287–300.
[13] C. Burkart, W. von Tümpling, T. Berendonk, D. Jungmann, Nanoparticles in wastewater treatment plants: a novel acute toxicity test for ciliates and its implementation in risk assessment, Environ. Sci. Pollut. Res., 22 (2015) 7485–7494.
[14] J.T.K. Quik, I. Velzeboer, M. Wouterse, A.A. Koelmans, D. van de Meent, Heteroaggregation and sedimentation rates for nanomaterials in natural waters, Water Res., 48 (2014) 269–79.
[15] M.R. Wiesner, G.L. Lowry, P. Alvarez, D. Dionysiou, P. Biswas, Assessing the risks of manufactured nanomateirals, Environ. Sci. Technol., 40 (2006) 4337–4345.
[16] N.-Q. Puay, G. Qiu, Y.-P. Ting, Effect of zinc oxide nanoparticles on biological wastewater treatment in a sequencing batch reactor, J. Cleaner Prod., 88 (2015) 139–145.
[17] P.K. Westerhoff, M.a. Kiser, K. Hristovski, Nanomaterial removal and transformation during biological wastewater treatment, Environ. Eng. Sci., 30 (2013) 109–117.
[18] C. Zhang, Z. Hu, P. Li, S. Gajaraj, Governing factors affecting the impacts of silver nanoparticles on wastewater treatment, Sci. Total Environ., 572 (2016) 852–873.
[19] P.A. Neale, Å.K. Jämting, B.I. Escher, J. Herrmann, A review of the detection, fate and effects of engineered nanomaterials in wastewater treatment plants, Water Sci. Technol., 68 (2013) 1440.
[20] M. Tan, G. Qiu, Y.-P. Ting, Effects of ZnO nanoparticles on wastewater treatment and their removal behavior in a membrane bioreactor, Bioresour. Technol., 185 (2015) 125–133.
[21] Y. Yang, Z. Yu, T. Nosaka, K. Doudrick, K. Hristovski, P. Herckes, P. Westerhoff, Interaction of carbonaceous nanomaterials with wastewater biomass, Front. Environ. Sci. Eng., (2015). doi:10.1007/s11783-015-0787-9.
[22] L. Hou, K. Li, Y. Ding, Y. Li, J. Chen, X. Wu, X. Li, Removal of silver nanoparticles in simulated wastewater treatment processes and its impact on COD and $NH_4$ reduction, Chemosphere, 87 (2012) 248–252.
[23] L. Hou, J. Xia, K. Li, J. Chen, X. Wu, X. Li, Removal of ZnO nanoparticles in simulated wastewater treatment processes and its effects on COD and $NH_4^+$-N reduction, Water Sci. Technol., 67 (2013) 254–260.
[24] S.K. Brar, M. Verma, R.D. Tyagi, R.Y. Surampalli, Engineered nanoparticles in wastewater and wastewater sludge - evidence and impacts, Waste Manage., 30 (2010) 504–20.
[25] V. Serrão Sousa, C. Corniciuc, M. Ribau Teixeira, The effect of $TiO_2$ nanoparticles removal on drinking water quality produced by conventional treatment C/F/S, Water Res., 109 (2017) 1–12.
[26] J. Olabarrieta, O. Monzón, Y. Belaustegui, J.-I. Alvarez, S. Zorita, Removal of $TiO_2$ nanoparticles from water by low pressure pilot plant filtration, Sci. Total Environ., 618 (2018) 551–560.
[27] R.J. Honda, V. Keene, L. Daniels, S.L. Walker, Removal of $TiO_2$ nanoparticles during primary water treatment: role of coagulant type, dose and nanoparticle concentration, Environ. Eng. Sci., 31 (2014) 127–134.
[28] C. Zhang, J. Lohwacharin, S. Takizawa, Effect of ions on removal of $TiO_2$ nanoparticles by coagulation and microfiltration, Environ. Eng. Sci., 35 (2018) 420–429.
[29] A. Popowich, Q. Zhang, X. Chris Le, Removal of nanoparticles by coagulation, J. Environ. Sci., 38 (2015) 168–171.
[30] L. Cumbal, A.K. SenGupta, Arsenic removal using polymer -supported hydrated iron(III) oxide nanoparticles: role of Donnan membrane effect, Environ. Sci. Technol., 39 (2005) 6508–6515.
[31] H.T. Wang, Y.Y. Ye, J. Qi, F.T. Li, Y.L. Tang, Removal of titanium dioxide nanoparticles by coagulation: effects of coagulants, typical ions, alkalinity and natural organic matters, Water Sci. Technol., 68 (2013) 1137–1143.
[32] Q. Sun, Y. Li, T. Tang, Z. Yuan, C.-P. Yu, Removal of silver nanoparticles by coagulation processes, J. Hazard. Mater., 261 (2013) 414–420.
[33] B. Xie, Z. Xu, W. Guo, Q. Li, Impact of natural organic matter on the physicochemical properties of aqueous C60 nanoparticles, Environ. Sci. Technol., 42 (2008) 2853–2859.
[34] S. Ghosh, H. Mashayekhi, P. Bhowmik, B. Xing, Colloidal stability of $Al_2O_3$ nanoparticles as affected by coating of structurally different humic acids, Langmuir, 26 (2010) 873–879.
[35] R. Chouari, D. Le Paslier, P. Daegelen, C. Dauga, J. Weissenbach, A. Sghir, Molecular analyses of the microbial community composition of an anoxic basin of a municipal wastewater treatment plant reveal a novel lineage of proteobacteria, Microb. Ecol., 60 (2010) 272–281.
[36] L. Zhang, J. Mao, Q. Zhao, S. He, J. Ma, Effect of $AlCl_3$ concentration on nanoparticle removal by coagulation, J. Environ. Sci., 38 (2015) 103–109.
[37] F. Ahmed, C.M. Santos, R.A.M. V. Vergara, M.C.R. Tria, R. Advincula, D.F. Rodrigues, Antimicrobial applications of electroactive PVK-SWNT nanocomposites, Environ. Sci. Technol., 46 (2011) 1804–1810.
[38] I.E. Mejías Carpio, C.M. Santos, X. Wei, D.F. Rodrigues, Toxicity of a polymer–graphene oxide composite against bacterial planktonic cells, biofilms, and mammalian cells, Nanoscale, 4 (2012) 4746.
[39] A. Amirtharajah, K.M. Mills, Rapid-mix design for mechanisms of alum coagulation, J. AWWA, 74 (n.d.) 210–216.
[40] AWWA, Water Quality and Treatment, 6th ed., McGraw-Hill, New York, 2011.
[41] S. Bykkam, R.K. Venkateswara, S.C. CH, T. Thunugunta, Synthesis and characterization of graphene oxide and its antibacterial activity against *Klebseilla* and *Staphylococus*, Int. J. Adv. Biotechnol. Res., 4 (2013) 1005–1009.
[42] L. Duan, R. Hao, Z. Xu, X. He, A.S. Adeleye, Y. Li, Removal of graphene oxide nanomaterials from aqueous media via coagulation: effects of water chemistry and natural organic matter, Chemosphere, 168 (2017) 1051–1057.
[43] Y.L.F. Musico, C.M. Santos, M.L.P. Dalida, D.F. Rodrigues, Improved removal of lead(ii) from water using a polymer - based graphene oxide nanocomposite, J. Mater. Chem. A, 1 (2013) 3789.
[44] K.A.D. Guzman, M.P. Finnegan, J.F. Banfield, Influence of surface potential on aggregation and transport of titania nanoparticles, Environ. Sci. Technol., 40 (2006) 7688–7693.
[45] M. Yan, D. Wang, J. Ni, J. Qu, C.W.K. Chow, H. Liu, Mechanism of natural organic matter removal by polyaluminum chloride: effect of coagulant particle size and hydrolysis kinetics, Water Res., 42 (2008) 3361–3370.
[46] J.E. Van Benschoten, J.K. Edzwald, Chemical aspects of coagulation using aluminum salts - I. Hydrolytic reactions of alum and polyaluminum chloride, Water Res., 24 (1990) 1519–1526.
[47] L. Chekli, M. Roy, L.D. Tijing, E. Donner, E. Lombi, H.K. Shon, Agglomeration behaviour of titanium dioxide nanoparticles in river waters: a multi-method approach combining light scattering and field-flow fractionation techniques, J. Environ. Manage., 159 (2015) 135–142.
[48] S.C. Smith, F. Ahmed, K.M. Gutierrez, D. Frigi Rodrigues, A comparative study of lysozyme adsorption with graphene, graphene oxide, and single-walled carbon nanotubes: potential environmental applications, Chem. Eng. J., 240 (2014) 147–154.
[49] S. Pasche, J. Vörös, H.J. Griesser, N.D. Spencer, M. Textor, Effects of ionic strength and surface charge on protein adsorption at PEGylated surfaces, J. Phys. Chem., B, 109 (2005) 17545–17552.
[50] J. Gregory, Particles in Water, Taylor & Francis, 2005.

**Supplementary information:**

**S1. Secondary effluent characteristics**

The secondary effluent used in the experiments was obtained as a grab sample from the Sims Bayou South Wastewater Treatment Plant (Houston, Texas, USA) (AHMED; RODRIGUES, 2013). The physical—chemical characteristics for the secondary effluent sample were: dissolved organic carbon, 37.3 mg $L^{-1}$; total chemical oxygen demand: 90.0 mg $L^{-1}$; pH: 7.0; turbidity: 5.5 NTU.

**S2. Graphene oxide (GO) synthesis and characterization**

Graphene oxide was synthesized from graphite (<20 μm, Sigma-Aldrich, USA) using the modified Hummers' oxidation method (HUMMERS; OFFEMAN, 1958). All the reagents were purchased from Sigma-Aldrich, except where noted. The nanomaterial was prepared as previously described (AHMED; RODRIGUES, 2013). The successful synthesis of graphene oxide was confirmed using Nicolet iS10 FTIR Spectrometer by identifying the following characteristics peaks in the spectrum: 3,379 ($cm^{-1}$) (hydroxyl, –OH stretching), 1,727 ($cm^{-1}$) (carboxylic, –COOH), 1,625 ($cm^{-1}$) (C=C) and 1,061 ($cm^{-1}$) (epoxy group) (CHEN et al., 2013; FAN; GRANDE; RODRIGUES, 2017).

Prior to any experimental dilution, a 30-min sonication step was used to homogenize the GO stock solution. GO concentrations of 1, 5 and 10 mg $L^{-1}$ were prepared in 1-L volume using DI water or wastewater secondary effluent. The concentrations were confirmed by absorbance, using quartz cuvettes, with a UV–Vis spectrometer (Synergy MX Microplate Reader, BioTek, USA) based on a modified protocol by Wang et al. (2010) (NGUYEN; RODRIGUES, 2018).

**S3. GO detection and calibration curve**

The highest peak of GO detection was λ = 230 nm, as previously described (SHIN et al., 2009; YANG et al., 2015; ZHANG et al., 2010). The calibration curve (Fig. S1 showed in this section) was obtained by mixing the GO with DI water in the following concentrations: 25, 10, 5, 2.5, 1.0 and 0.1 mg $L^{-1}$. These concentrations were used for the calibration curve since it covers the entire range of the GO used in this study. The absorbance for each concentration was plotted and a standard curve was generated. The resulted equation used to calculate concentration of GO solution and GO removal was: $y = 0.0361x + 0.0057$; $R^2 = 0.9976$.

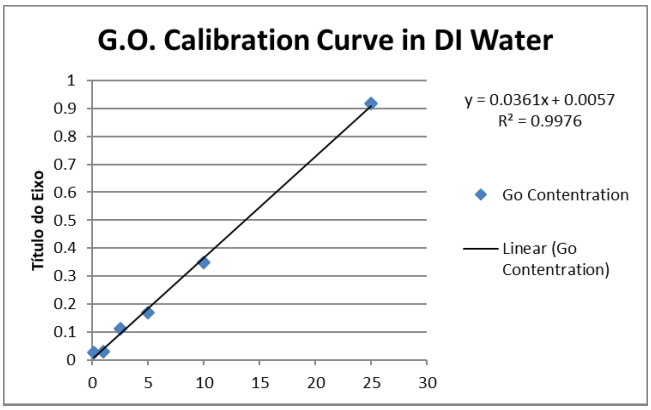


Fig. S1. Calibration curve.

**S4. Solutions of coagulants**

For calculations of PAC solutions, the coagulant was understood as $Al_2(SO_4)_3{\cdot}16H_2O$ and, based on literature, treated in terms of $Al^{+3}$ ions, which is the active form of aluminum. The stock solution was obtained at concentration of 1.87 g $Al^{+3}$ $L^{-1}$. The ferric chloride ($FeCl_3$), obtained in solid form, was diluted to obtain a coagulant stock solution of 2.07 g $Fe^{+3}$ $L^{-1}$. From the stock solutions, dilutions were prepared to achieve a final concentrations of 2.07, 3.14 and 6.21 mg $Fe^{+3}$ $L^{-1}$ and 1.87, 3.74 and 5.61 mg $Al^{+3}$ $L^{-1}$ in the samples prior to the jar test. More information on coagulant dosage and chemistry can be found at (LETTERMAN, R. D. YIACOUMI, 2011).